Multi-robot Mapping of Lava Tubes

X. Huang, J. Yang, M. Storrie-Lombardi, G. Lyzenga, C. M. Clark

Abstract Terrestrial planetary bodies such as Mars and the Moon are known to harbor volcanic terrain with enclosed lava tube conduits and caves. The shielding from cosmic radiation that they provide makes them a potentially hospitable habitat for life. This motivates the need to explore such lava tubes and assess their potential as locations for future human outposts. Such exploration will likely be conducted by autonomous mobile robots before humans, and this paper proposes a novel mechanism for constructing maps of lava tubes using a multi-robot platform. A key issue in mapping lava tubes is the presence of fine sand that can be found at the bottom of most tubes, as observed on earth. This fine sand makes robot odometry measurements highly prone to errors. To address this issue, this work leverages the ability of a multi-robot system to measure the relative motion of robots using laser range finders. Mounted on each robot is a 2D laser range finder attached to a servo to enable 3D scanning. The lead robot has an easily recognized target panel that allows the follower robot to measure both the relative distance and orientation between robots. First, these measurements are used to enable 2D (SLAM) of a lava tube. Second, the 3D range measurements are fused with the 2D maps via ICP algorithms to construct full 3D representations. This method of 3D mapping does not require odometry measurements or fine-scale environment features. It was validated in a building hallway system, demonstrating successful loop closure and mapping errors on the order of 0.63 meters over a 79.64 meters long loop. Error growth models were determined experimentally that indicate the robot localization errors grow at a rate of 20 mm per meter travelled, although this is also dependent on the relative orientation of robots localizing each other. Finally, the system was deployed in a lava tube located at Pisgah Crater in the Mojave Desert, CA. Data was collected to generate a full 3D map of the lava tube. Comparison with known measurements taken between two ends of the lava tube indicates the mapping errors were on the order of 1.03 m after the robot travelled 32 meters.

Xin Huang, Jingbin Yang, Michael Storrie-Lombardi, Gregory Lyzenga, Christopher M. Clark
Harvey Mudd College, Claremont, California 91711 e-mail: {xhuang, jyang, mstorrielombardi, lyzenga, clark}@hmc.edu

1 Introduction

It is understood that within our solar system, Mars shares an environment similar in many respects to that of Earth, and it is possible that there might exist traces of life. The surface of Mars is relatively inhospitable and is constantly bombarded by cosmic radiation due to the thin atmosphere and lack of planetary magnetic field. Furthermore, the surface temperature ranges from 160 Kelvin to 215 Kelvin from the equator to the poles. The temperature also fluctuates greatly within a day. The upper few kilometers of the lithosphere are likely to be frozen, with the exception of volcanically active areas. Despite these harsh conditions, many scientists predict the existence of a saline groundwater system in the shallow subsurface of the planet, and therefore the subsurface may provide or may have provided a suitable environment for life. NASA's Astrobiology Roadmap objectives include investigating biosignatures in subsurface rocks, modeling subsurface habitable environments, and developing robotic drilling systems to access subsurface environments on Mars [7].

Lava tubes on Mars have gained considerable interest in the astrobiological community because they offer protection from the harsh conditions experienced on the planet's surface. There have been many attempts to characterize these lava tubes to determine the best sites for future exploration and to study the geomicrobiology in lava tubes. To achieve these goals remote-sensing techniques are required [7]. The lava tubes often have many openings, uneven terrain and variation in floor texture. Therefore, while radar instruments have already been used to drill to the subsurface to detect such characteristics, existing sensing methods often lack the resolution necessary to detect exact positions of interest in each individual lava tube.

These challenges motivate the goal of developing autonomous robots that can explore lava tubes and conduct in-situ scientific measurements. Such robots would need to construct 3D maps of the tubes to not only allow the robot to localize in-situ sample measurements with respect to a coordinate frame fixed to the tube, but also to enable the robot to localize itself with respect to the tube and carry out autonomous robot navigation.

Constructing 3D maps with robots has been well studied in the Simultaneous Localization and Mapping (SLAM) community. Many SLAM strategies have used a single robot that fuses odometry and range measurements via filtering algorithms to localize the robot and map the environment [1, 8]. While these methods are reliable, they are limited by the conditions of the exploration environment. The susceptibility of the encoder odometry measurements to error resulting from the fine sand found on the lava tube floor further challenges the SLAM problem.

Proposed here is a multi-robot mapping framework that allows robots to cooperatively map lava tubes which a) have poor odometry measurements due to the fine sand of the tube floor, and b) lack fine-scale features that reduce dead reckoning errors. Section 2 of this paper presents related work. A three-step solution called *Platoon SLAM* is proposed in Section 3, where in the first two steps range finder measurements of the relative distance and bearing-angle orientations between robots are used to update their positions, and in the last step these updated positions

(a) (b)

Fig. 1: Image of the Jaguar robot (a) at the entrance of a lava tube (b) on the sandy ground

are used to seed ICP algorithm queries, that both localize the robot in 2D and construct maps in 3D. Implementation of these techniques are documented in Section 4, where results from hallway and lava tube mapping scenarios are presented. Finally, conclusions from these results are drawn in Section 5 and possible future work is proposed in 6.

2 Background

The problem of Simultaneous Localization and Mapping (SLAM) involves constructing a map of an unknown environment while localizing the position of the robot. SLAM is a maturing research area, with work most related to this project including advancements made in the sub-disciplines of 3D SLAM, ICP, 3D mapping in tube like structures, and multi-robot 3D SLAM.

A variety of approaches to 3D mapping in SLAM have been implemented that combine different localization and mapping techniques. Initially, 3D maps were built using multiple 2D scanners with different orientations to construct the 3D map. Thrun et. al. [11] used measurements from two laser scanners, oriented perpendicular with respect to each other to form 3D point clouds. However other methods mentioned below give higher resolution of the generated 3D map, including visual SLAM using cameras or 3D range sensing methods are used in autonomous mapping [3, 8, 14, 15, 24, 6]. One popular 3D scanning method uses a pair of cameras with RGB-D cameras in 3D sensing [6]. This method is not well suited for the low lighting environments and low power requirements encountered during the exploration. The more common sensing method is to use 3D laser range finders. These laser range finders are commonly made by spinning the 2D laser scanner to obtain 3D data in the form of 3D point clouds [3, 8, 24, 14]. There are also several attempts to combine a 3D sensor with a 6D localization method. Nuchter et. al. used a 3D scanner in combination with 6DOF IMU data to produce an error-minimized map

[8]. Borrmann et al [2] provides a detailed summary of current advancements in SLAM using 2D and 3D scanning mechanisms and explores 6D SLAM with scan matching.

There exist different techniques to register the point clouds into a 3D map, including 3D-FFT methods [21]. The registration currently used in this work, Iterative Closest Point (ICP), is one of the most common ways to register point clouds to represent maps in 3D space. Developed by Besyl et al and Chen et al [22, 23], it has been used in many occasions to register 3D maps [11, 8, 16]. There have also been findings on improvements for ICP in terms of processing, such as the 2D-NDT and 3D-NDT method [17], where the data is stored after computing in normal distributions. In addition, there are alternatives for ICP as described by Fischer et al [18] and Pathak et al [19] for pose registration which are not as commonly used.

Single robot 3D SLAM demonstrating successful loop closure in underground mine mapping started with Schedling [10]. These mines are similar to lava tubes in that they are long, winding, and without line-of-sight to GPS satellites. Huber et al [15] used a high resolution 3D scanner on a cart to create an 3D map of an underground mine without additional sensors. Nuchter el. al. also used multiple 3D SICK scanners in a stop-and-go method on robots to localize the robot and create a map of the environment through scan matching with ICP with point clouds [8]. Zlot et al used an iterative matching algorithm to first construct an open-loop map of the mine tunnel, and then a closed loop model [14]. The method relies on pose measurement data and uses a global registration algorithm instead of landmark detection for localization.

Multi-robot systems offer increased spatio-temporal coverage which can be leveraged when exploring and mapping unknown environments [5]. For example, Burgard's group had individual robots simultaneously explore different regions of an unknown environment. The work employed a probabilistic approach for the coordination of multiple robots to reduce the overall exploration time. An algorithm for multi-robot SLAM with sparse extended information filters was presented in Thrun's work [12]. The alignment of local maps into a single global maps was achieved by a tree-based algorithm that searches for similar-looking local landmark configurations. More relevant to this project is the work done by Rekleitis, where a pair of robots observe each other, and act in concert to reduce odometry errors [9]. However, this method relies on video camera observations, which is not suitable for underground lava tubes mapping.

3 Platoon SLAM

The goal of this work is to map the 3D environment of a lava tube using two robots equipped with 2D laser range finders. The lava tubes of interest are greater than 20 meters in length, and range in height between 0.30 and 3.0 meters. The tube walls are unpredictable, lacking sharp distinct corners. The tube floor consists of fine sand that causes encoder measurements to be highly unreliable due to slipping. Low light conditions in the mapping environment cause image processing techniques to require structured lighting that may increase payload weight and power consumption. Due to the shielding property of the lava tubes, no radiation communication such as GPS can be established between the robots in the tubes and the outside world. Therefore, a local-based SLAM solution is required.

Our core approach to this problem, called *Platoon SLAM*, uses two robots to navigate through the lava tube in a lead-follower formation. Each robot is equipped with a 2D laser range finder mounted on a servo to enable 3D range scanning. The lead robot will also have an easily observed target panel that can be detected by the follower robot's laser range finder. The primary role of the lead robot is to take 3D scans of the environment. The role of the follower robot is to measure the relative position and orientation changes of the robots as they traverse the length of the tube.

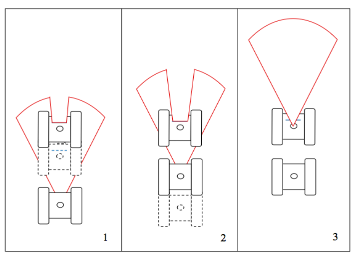

Fig. 2: Three step sequence: 1) lead robot moves and its state change is measured, 2) follower robot moves and its state change is measured, and 3) lead robot takes a 3D scan.

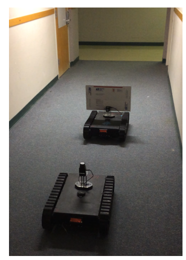

Fig. 3: Image of a two-robot system. The robots are Dr. Robot Jaguar Lite platforms. The lead robot is equipped with a target panel.

Fig. 4: A robot-obtained laser scan taken from the lava tube.

3.1 Platoon Actions

The two robots are tightly synchronized to repeat a sequence of 3 actions depicted in Fig. 2. In step 1, the lead robot moves forward a set distance and then the follower robot takes a stationary laser scan to detect the target panel on the lead robot. This scan measures the relative position of the lead robot. In step 2, the follower robot moves forward to a location just behind the lead robot. The follower robot again scans and detects the target panel to measure the relative position of the lead robot. In step 3, the lead robot takes a stationary 3D scan of the environment.

3.2 Robot Position Measurements

Steps 1 and 2 of the action sequence are used to obtain accurate measurements of the robots as they move forward to explore the lava tube. The follower robot obtains laser scans similar to that depicted in Fig. 4. The target panel is easily recognized in the center of this scan and is detected by an algorithm that searches for similar consecutive range measurements. The output of this algorithm is a series of range and bearing tuples $[\rho_i, \alpha_i]$ associated with reflections from the lead's target panel. Here ρ_i represents the relative distance between the two robots and α_i represents the relative bearing angle of the lead robot with respect to the follower robot, as shown in Fig. 5. Each $[\rho_i, \alpha_i]$ tuple is taken with respect to the follower robot's coordinate frame and can be converted to the relative position $[\Delta x_i, \Delta y_i]$ within this local frame. The mean relative position $[\bar{\Delta} x, \bar{\Delta} y]$ can be calculated and used to determine a mean relative range and bearing $[\bar{\rho}, \bar{\alpha}]$ from the follower to the lead robot.

To calculate the yaw angle θ_L of the lead robot in the global frame, the difference in bearing angles between the two robots ϕ must first be extracted as the arctangent of the slope of the line fit to the $[\Delta x_i, \Delta y_i]$ tuples. Then, for the first step of the t^{th} action sequence, the lead robot's state $[x_L\ y_L\ \theta_L]_t^T$ can be updated from the follower robot's previous state $[x_F\ y_F\ \theta_F]_{t-1}^T$:

$$\beta = \bar{\alpha} + \theta_F - \frac{\pi}{2} \tag{1}$$

$$\begin{bmatrix} x_L \\ y_L \\ \theta_L \end{bmatrix}_t = \begin{bmatrix} x_F \\ y_F \\ \theta_F \end{bmatrix}_{t-1} + \begin{bmatrix} \bar{\rho}\cos\beta \\ \bar{\rho}\sin\beta \\ \phi \end{bmatrix}_t \tag{2}$$

In Equations (1) and (2), β is the angle of the ray connecting the follower to the lead robot, as calculated with respect to the global coordinate frame. Fig. 5 depicts the geometry of these calculations.

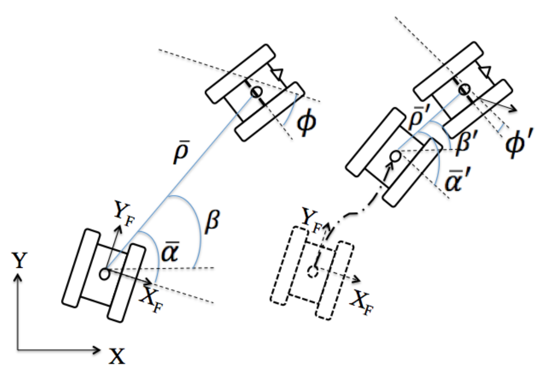

Fig. 5 Geometric representations for steps 1 and 2 of one sequence

For the second step of the t^{th} action sequence, the follower robot's state $[x_F\ y_F\ \theta_F]_t^T$ can be updated after its forward movement using its detection of the lead robot's target. In this case, the target data produces similar measurements to the first step, but we denote the second step measurements with $'$, i.e. $\bar{\rho}', \bar{\alpha}', \beta', \phi'$.

$$\beta' = \bar{\alpha}' + \theta_L - \frac{\pi}{2} \tag{3}$$

$$\begin{bmatrix} x_F \\ y_F \\ t_F \end{bmatrix}_t = \begin{bmatrix} x_L \\ y_L \\ t_L \end{bmatrix}_t - \begin{bmatrix} \bar{\rho}' \cos\beta' \\ \bar{\rho}' \sin\beta' \\ \phi' \end{bmatrix} \tag{4}$$

The proposed solution assumes the lead robot's target can always be detected by the follower robot. This can be achieved by ensuring the lead robot takes relatively small steps forward and by subsequently modifying the pitch angle of the follower's 2D laser range finder until the target is detected within a 2D scan.

3.3 Robot Localization

Once the robot state updates are calculated using inter-robot range and bearings as described in Equation (2) and Equation (4), the robot states are further refined using environment range measurements. This refinement, or correction, is accomplished using a method called Iterative Closest Point (ICP). ICP attempts to find the relative transformation between two data sets. In this case, each data set corresponds to a single 3D scan taken by the lead robot during step 3. The scan consists of 3D points indicating the position of the lava tube contour with respect to the lead robot. Hence if the ICP algorithm is applied to two consecutive 3D scans taken by the lead robot, the algorithm will output a transformation that represents the lead robot's movement between the consecutive scans.

To initialize the ICP algorithm, an estimate of the transformation between lead robot scans is required. In this case, the relative movements calculated in Section 3.2, e.g. $x_{L,t} - x_{L,t-1}$, are used to initialize the ICP algorithm. To reduce the run time complexity, ICP is conducted only on the range data points that lie within some threshold of the horizontal plane that intersects with the robot sensor, as the elevation change between two consecutive scan positions is relatively small. To determine the horizontal plane, IMU data is used to calculate the roll and pitch angles of the robot relative to the initial pose of the robot to which the origin of the global coordinate frame is anchored.

The effect of running the 2D ICP implementation is illustrated in Fig. 6a and Fig. 6b, where the points clouds (blue) from two scans are plotted. The red and pink dots indicate the points determined to be within the 2D horizontal plane of two consecutive 3D scans. It is clear that running ICP to refine the position of the two 3D scans in Fig. 6a improves the alignment of the two subsequent scans in Fig. 6b, with pink dots and red dots overlapping.

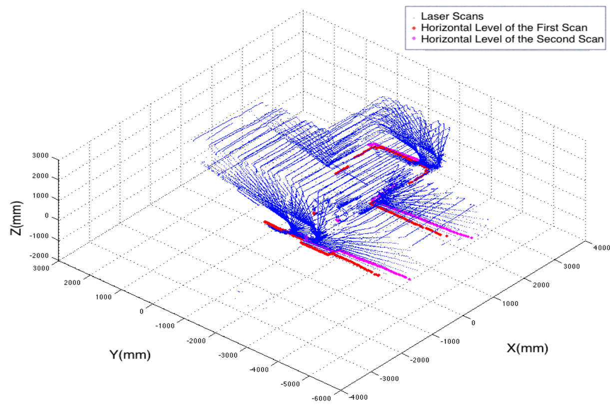

(a)

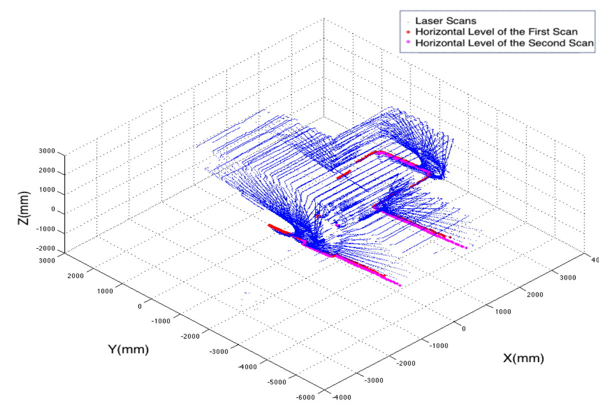

(b)

Fig. 6: Two consecutive point clouds (a) before registration (b) after registration

3.4 Lava Tube Mapping

As described in the previous two sections, the first two steps in the 3 step sequence are used to estimate the lead robot's state at every 3D scan location with respect to a global coordinate frame. In last step, where the lead robot obtains a 3D scan of the environment, data is collected for constructing the 3D map of the lava tube. Each 3D scan produces a 3D point cloud that is added to the map to create a single global point cloud map representing the entire lava tube. After each scan, the positions of two robots are updated according to point registration results by ICP.

4 Experiments

In this section, experimental results are presented that validate the ability of *Platoon SLAM* to demonstrate loop closure while mapping a hallway system of known dimensions, allow for modeling error growth using the *Platoon SLAM* methodology in environments with sandy terrain, and demonstrate the ability of a robot pair to map a lava tube located at Pisgah Crater in the Mojave Desert, CA.

All experiments were conducted using two Dr. Robot Jaguar Lite platforms (see Fig. 3). The Jaguar Lite Platform is a differential drive tracked vehicle equipped with a 5Hz GPS, wheel encoders, a color camera (640x480, 30fps), two header lights, a 9DOF IMU from Razor and a Hokuyo laser scanner (20-4000mm with 3% error). The laser scanner is attached to a servo so that it could be tilted to obtain 3D laser data. It is designed for both indoor and outdoor navigation and is able to navigate through various terrains such as sand, rock, concrete, grass and gravel. Each platform is powered by a 6-cell LiPo battery with a maximum operating time of 4 hours.

4.1 Structured Environment Mapping

The first set of experiments was used to assess mapping ability in a controlled and structured environment. Two robots travelled around a rectangular hallway, the total length of which is 79.64 meters with 21.96 meters in width and 17.86 meters in height. The lead robot took a total of 85 scans, with approximately 1 meter travelled between consecutive scans, and returned to its starting point at the end of the experiment. Sample maps produced with the logged data set are shown in Fig. 7a. After 80 meters' travel, the error associated with the final lead robot position was approximately 5 meters when ICP was not used to refine the state estimate. When the ICP was applied to improve the localization error, the end position estimation error was reduced to 0.63 meters. The hallway map created by ICP has a mean estimated width and height of 22.59 meters and 17.91 meters respectively. Image of the 2D localization conducted with ICP is shown in Fig. 7b. It can be observed that using ICP allows for loop closure. The loop closure occurs when a new point cloud, after being registered to its previous scan, finds a second matched point cloud among the earlier recorded point clouds.

4.2 Error Model and Lava Tube Mapping

To model the error growth as a function of distance travelled by the platoon, the actual and measured relative positions between two robots were logged. Two robots were placed in a sand pit located near Harvey Mudd College. The lead robot was fixed at a stationary location, and the follower robot was placed (and replaced 4

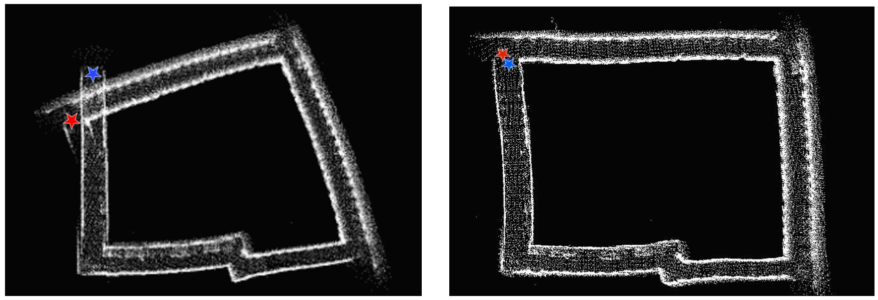

(a) (b)

Fig. 7: Hallway map (a) created with multi-robot SLAM (b) after corrected by ICP. The robots started at blue star and stopped at red star.

times) at 49 different positions in the sand pit. The measurement error, calculated by taking the difference between estimated and real distances for each position, is shown in Fig. 8, where a 4th order function has been used to model the estimation error as a function of the follower robot's relative position and angle. It can be seen that the error remains low (on the order of 0.02 m) when the relative distance is less than 2.5 m and the relative angle is less than 30 degrees between two robots.

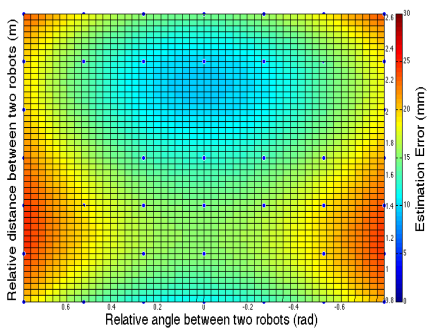

Fig. 8: Estimation error as a function of relative position and relative angle between two robots on the sand pit.

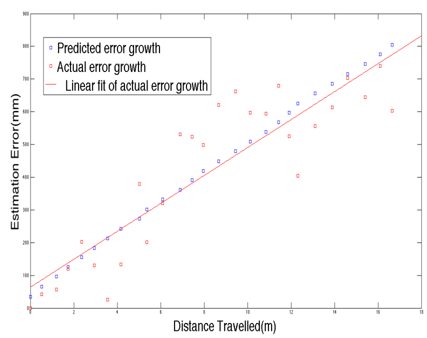

Fig. 9: Predicted error growth and actual error growth *vs*. distance travelled. The actual error growth is modeled by a linear fit (red line).

This model can be propagated over a series of scans to determine error growth as a function of distance travelled. In the same sand pit, the lead and follower robots were driven to follow a rectangular path. The real error growth and model predicted error growth have been plotted in Fig. 9. It can be seen that the actual error growth modeled by a linear fit is predicted by the error propagation function.

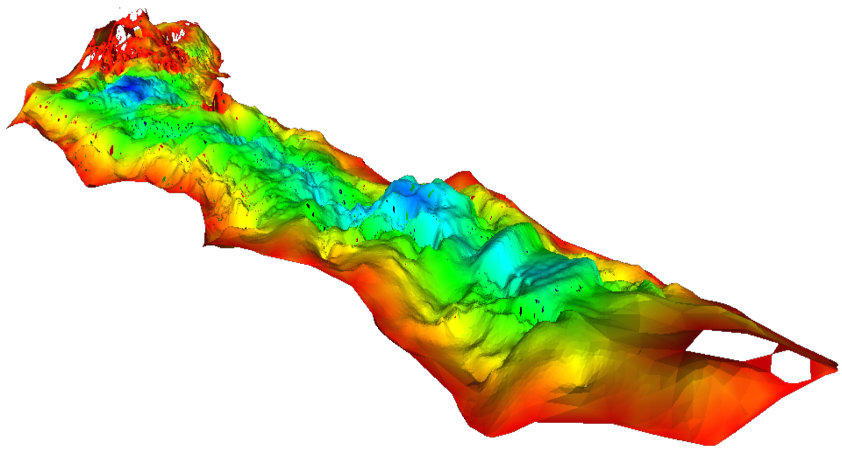

Fig. 10: Top view of the lava tube ceiling model in a top isometric view.

4.3 Lava Tube Mapping

Final experiments were conducted in lava tubes located at Pisgah Center in the Mojave Dessert, CA. The tubes are shielded from external radiation by thick walls of lava rock. The main tube explored is 0.30 to 3 meters high, 2 to 4 meters wide, 32 meters long, and 6 meters down to the dessert surface. The elevation change of the tube ground is no more than 0.5 meter. The temperature inside the tube during summer is about 25 °C while the surface temperature is 40 °C. There is almost no light in the tube. The ceiling consists of near vertical rocks with irregular features that are difficult to characterize. The floor is covered with fine silica sand and rocks, which makes it easy for the tread wheeled robot to slip. In this tube, two robots started at one end of the tube and navigated to the other end. The robot camera could not see anything with the header lights on due to the poor lighting conditions. The maximum pitch change relative to horizontal plane was no larger than 20 degree. The lead robot took 37 scans in 40 minutes to construct the map shown in Fig. 10. Using the map, the total length of the tube is 30.97 meters which is just over 1 meter less than the actual length measured by GPS data.

4.4 Lessons Learned

Several lessons were learned from the lava tube deployment. First, it is important to protect the robot platform against sand. During the experiment, it was found that the fine sand penetrated the robot parts as well as accumulated on the tracks. In consequence, the robot track had increased slipping, slower movement and fast odometry error growth, as shown in Fig. 11. Thus it is suggested that all holes on the robots and laptops should be covered, all screws should be tightened, and the track should be cleaned up before each experiment. As well, in order to reduce slip and increase travel speed, a track spoke with larger diameter is recommended, since it will add more contacting area between the track surface and ground.

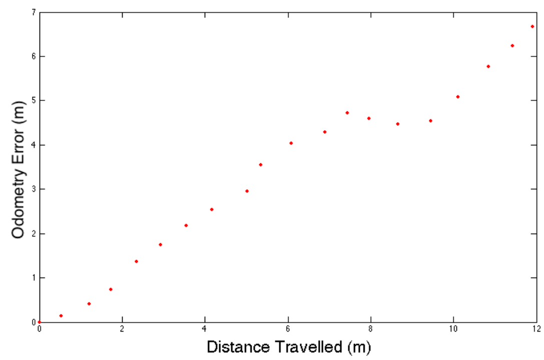

Fig. 11 Odometry estimation error as a function of distance travelled on the sand pit.

The battery life is a crucial resource during the experiment, as it is hard to charge the battery in the middle of the dessert or on Mars. Therefore, in order to save battery life, efficient and faster algorithms are recommended for the robot control system. The team used 2D ICP instead of 3D ICP to register point clouds for this reason. Also, it was mentioned earlier that the team tilted the 2D laser scanner to obtaining 3D point clouds. The tilt step size was determined to be 5 degrees. A smaller step size will take longer time to obtain data and thus require more battery source, and a larger step size will lose information when constructing the map. Therefore, the step size needs to be carefully selected.

5 Conclusions

Presented in this paper is a multi-robot approach to mapping lava tube environments on sandy floors that yield inaccurate robot odometry measurements without fine scale features. The approach, termed *Platoon SLAM*, involves an iterative 3 step process where robots coordinate their actions to allow them to capture 3D range scans and measure the relative transformations between scans. These transformation measurements are refined with an ICP algorithm. To construct 3D maps, the 3D scans are translated to point clouds that are added to a global map. The maps created with this system demonstrate error growth on the order of 3% per meter travelled. Mapping loop closure was successfully demonstrated in a hallway system of approximately 80 meters in length. A map of a lava tube located in Mojave Desert was created and the tube length was estimated to be 30.97 meters when the actual length was 32 meters.

6 Future Work

Future work involves implementing autonomous path planning. One important assumption in our solution is that the lead robot's target can always be detected by the follower robot. This requires a path planning algorithm that ensures the relative position and orientation between two robots are within some threshold to minimize error growth. The function calculated in Section 4 suggests using movements with less than 2.5 meters in distance and less than 30 in degrees relative orientation between robots. The height of the lava tube along the planned path should also be considered in the algorithm so that both robots can pass through the tube. This can be achieved by analyzing the 3D map generated by the lead robot.

Additional work includes occupancy grid map generation. Currently a mesh file is created as the 3D map. This can be helpful for determining the shape and size of the lava tube. However, with an occupancy grid map, control parameters such as resolution, memory, as well as complexity can be controlled so maps can be generated according to different circumstances and restrictions. Additionally, as many off-the-shelf algorithms use an occupancy grid map representation, it will give future researchers more leverage after they map the environment.

The current work can be easily extended to more than two robots. The follower robots in the platoon will be able to provide more 3D scans and thus produce a more accurate map by advancing through the lava tube in the platoon manner. Specifically, point clouds generated from each robot can be matched and then merged together to increase map accuracy.

The ultimate goal for this project will be moving towards autonomous multi-robot 6DOF SLAM in lava tubes. For the robot system to be able to navigate on steep slopes, the follower robot should have 3D scanning capabilities to detect the target panel on the lead robot on terrains with significant changes in slope. To be able to localize with a 6DOF state, IMU data will likely be needed to further integrated to the state estimation of the robot system.

Acknowledgements The authors would like to thank all the people who contributed to the project: Samuel Yim, Shreyasha Paudel, Phuong Nguyen, Sean Messenger and Kevin Smith.

References

1. Aulinas, J. et al (2008) The SLAM problem: a survey. Proceedings of the 2008 conference on Artificial Intelligence Research and Development: Proceedings of the 11th International Conference of the Catalan Association for Artificial Intelligence:363-371.

2. Borrmann, D. et al (2008) Globally consistent 3D mapping with scan matching. Robotics and Autonomous Systems (Volume: 56, Issue: 2):130-142.
3. Bosse, M et al (2009) Continuous 3D Scan-Matching with a Spinning 2D Laser. Robotics and Automation, 2009. ICRA '09. IEEE International Conference on:4312-4319.
4. Burgard, W. et al (2000) Collaborative Multi-Robot Exploration. Robotics and Automation, 2000. Proceedings. ICRA '00. IEEE International Conference on (Volume:1):476 - 481.
5. Fenwick, J et al (2002) Cooperative concurrent mapping and localization. Robotics and Automation, 2002. Proceedings. ICRA '02. IEEE International Conference on (Volume:2):1810-1817
6. Henry, P. et al (2014) RGB-D Mapping: Using Depth Cameras for Dense 3D Modeling of Indoor Environments. Experimental Robotics, Springer Tracts in Advanced Robotics 79:477-491.
7. Leveille R et al (2012) Lava tubes and basaltic caves as astrobiological targets on Earth and Mars: A review. Planetary and space science 58:592.
8. Nutcher H. et al (2007) 6D SLAM-3D Mapping Outdoor Environments. Journal of Field Robotics 24:699-722.
9. Rekleitis I, Dudek G and Milios E (2001) Multi-robot collaboration for robust exploration. Annals of Mathematics and Artificial Intelligence 31:7-40.
10. Scheding, S (1997) Experiments in autonomous underground guidance. Robotics and Automation, 1997. Proceedings., 1997 IEEE International Conference on (Volume:3):1898 - 1903.
11. Thrun, S. et al (2000) A Real-Time Algorithm for Mobile Robot Mapping With Applications to Multi-Robot and 3D Mapping. Robotics and Automation, 2000. Proceedings. ICRA '00. IEEE International Conference on (Volume:1):321 - 328.
12. Thrun, S et al (2004) Simultaneous Localization and Mapping With Sparse Extended Information Filters. Algorithmic Foundations of Robotics V 7:363-380
13. Tong, C et al (2012)Three-dimensional SLAM for mapping planetary work site environments. Journal of Field Robotics 29:381-412.
14. Zlot R., Bosse M. (2012) Efficient Large-Scale 3D Mobile Mapping and Surface Reconstruction of an Underground Mine. Field and Service Robotics:Springer Tracts in Advanced Robotics 92:479-493.
15. Huber D. F., Vandapel N. (2006) Automatic Three-dimensional Underground Mine Mapping. IJRR (Volume 25, No.1):7-17.
16. Pomerleau F.et al (2013) Comparing ICP Variants on Real-World Data Sets. Autonomous Robots (Volume 34, No. 3):133-148
17. Magnusson, M. et al (2007) Scan registration for autonomous mining vehicles using 3D-NDT. Journal of Field Robotics 10(24): 803-827.
18. Fischer, D., Kohlhepp, P. (2000). 3D geometry reconstruction from multiple segmented surface descriptions using neuro-fuzzy similarity measures. Journal of Intelligent and Robotic Systems, 29(4), 389-431.
19. Pathak K. et al (2010) Fast Registration Based on Noisy Planes with Unknown Correspondences for 3D Mapping. IEEE Transactions on Robotics 26:424-441.
20. Vaskevicius N. et al (2010) Efficient Representation in 3D Environment Modeling for Planetary Robotic Exploration. Advanced Robotics 24:1169-1197.
21. Lucchese L. et al (2002) A frequency domain technique for range data registration. IEEE Transactions on Pattern Analysis and Machine Intelligence 24: 1468-1484.
22. Besl, P. J. et al (1992). Method for registration of 3-D shapes. In Robotics-DL tentative (pp. 586-606). International Society for Optics and Photonics.
23. Chen, Y et al(1991). Object modeling by registration of multiple range images. In Proceedings of the IEEE international conference on robotics and automation:27242729
24. Weingarten, J et al (2005). EKF-based 3D SLAM for structured environment reconstruction. In Intelligent Robots and Systems, 2005.(IROS 2005). 2005 IEEE/RSJ International Conference on: 3834-3839. IEEE.